Zirconium–Sulfur Chemistry. Synthesis and Structural Characterization of the $Zr_3S_3(^tBuS)_2(BH_4)_4(THF)_2$, $Zr_6S_6(^tBuS)_4(BH_4)_8(THF)_2$, $Zr_3(S)(^tBuS)_{10}$, and $(Mg(THF)_6)[Zr_2(SPh)_{7.2}(CH_2Ph)_{1.8}]_2\cdot 3THF$ Clusters. Activation and Cleavage of the C–S Bond in Zirconium-Coordinated Alkanethiolate Ligands

D. Coucouvanis,* A. Hadjikyriacou, R. Lester, and M. G. Kanatzidis

Department of Chemistry, The University of Michigan, Ann Arbor, Michigan 48109-1055

Received December 15, 1993®

New zirconium thiolate complexes have been obtained by the acidification of either the $Zr(BH_4)_4$ or the $Zr(CH_2Ph)_4$ complexes by RSH molecules in reactions that produce either B_2H_6 or toluene as byproducts. The polynuclear clusters $Zr_3S_3(^tBuS)_2(BH_4)_4(THF)_2$, **I**, and $Zr_6S_6(^tBuS)_4(BH_4)_8(THF)_2$, **II**, are obtained from ^{t}BuSH and $Zr(BH_4)_4$. The $Zr_3(S)(^tBuS)_{10}$ cluster, **III**, is obtained from ^{t}BuSH and $Zr(CH_2Ph)_4$. The sulfido ligands in these clusters are obtained from the zirconium-coordinated $^tBuS^-$ ligands as a result of C–S bond activation followed by what appears to be mainly a heterolytic bond cleavage reaction. The $(Mg(THF)_6)[Zr_2(SPh)_{7.2}(CH_2Ph)_{1.8}]_2\cdot 3THF$ cluster, **IV**, was obtained from $Zr(CH_2Ph)_4$ and PhSH in the presence of $H_2CPhMgCl$. The absence of S^{2-} ligands in IV is attributed to a stronger C–S bond in the Z-coordinated PhS^- ligands. The compounds **I–IV** crystallize all in the space group $P2_1/c$. The cell dimensions are a = 11.545(3) Å, b = 16.481(4) Å, c = 18.118(4) Å, and β = 91.23(2)° for **I**, a = 12.443(1) Å, β = 15.197(2) Å, c = 18.365(2) Å, and β = 70.214(7)° for **II**, a = 22.009(8) Å, b = 11.372(4) Å, c = 26.980(7) Å, and β = 101.93(3)° for **III**, and a = 14.352(6) Å, b = 22.307(14) Å, c = 23.554(8) Å, and β = 95.46(3)° for **IV**. The data for all structures were obtained on an automatic diffractometer employing Mo Kα radiation. Full matrix refinement of 235 parameters on 2169 data for **I**, 278 parameters on 3102 data for **II**, 315 parameters on 3966 data for **III**, and 387 parameters on 2582 data for **IV** gave final R_w values of 0.050, 0.043, 0.069, and 0.070, respectively. The structures of **I–III** are closely related and contain the $[Zr_3(\mu_3\text{-}S)_2(\mu_2\text{-}S)_3]^{n+}$ core, with a distorted hexagonal bipyramidal structure, as a structural feature. In **I** and **II** the Zr_3 subunits (n = 4) show two μ_2-^{t}Bu thiolates and a μ_2-sulfide ligands bridging the Zr atoms in the equatorial plane and two μ_3-sulfido ligands serving as "capping" ligands on the axial positions. In **III** (n = 6) three μ_2-^{t}Bu thiolates bridge the Zr atoms in the equatorial plane and μ_3-sulfido and μ_3-thiolato ligands serve as "capping" ligands on the axial positions. The coordination geometries of the Zr atoms are distorted octahedral, and in **I** and **II** BH_4^- and THF ligands are involved in coordination. Only sulfur ligands are coordinated to the zirconium atoms in **III**.

Introduction

Reactivity studies on the chemistry of specific groups in various thio- and oxothiomolybdate complexes[1] have revealed the Mo=S chromophore as a reactive site that undergoes addition reactions with activated alkynes,[1a,b] carbon disulfide,[2] and sulfur dioxide.[3] As suggested previously by theoretical calculations,[4] this reactivity is more pronounced in the presence of a "spectator" Mo=O group and at times leads to self-coupling reactions. In search for an even more reactive M=S chromophore we initiated our studies toward the synthesis of Zr/S coordination complexes that might eventually lead to the Zr=S chromophore or following self-coupling reactions to polynuclear derivatives. The rarity of soluble polynuclear Zr clusters and the potential importance of such species in small-molecule activation and reduction[5] prompted us to examine the methodology for the synthesis of such compounds.

The coordination chemistry of zirconium with sulfur ligands is rather limited. In addition to the complexes reported in this work, other known Zr/S coordination compounds include the octahedral dithiolene $[(Zr(L)_3]^{2-}$ complexes[6] (L = $[S_2C_6H_3CH_3]^{2-}$ or $[S_2C_6H_4]^{2-}$), the eight-coordinate dithiocarbamate complexes[7] $Zr(R_2Dtc)_4$, and the pentagonal bipyramidal $(Cp)Zr(Me_2Dtc)_2$ complex.[8] More recently the syntheses and structural characterization of $[(\eta^5\text{-}C_5H_5)(CO)_3W](\mu\text{-}S)[Zr(Cl)(\eta^5\text{-}C_5H_5)_2$,[9] the $[(Cp_2Zr]_2(\mu\text{-}S)_2$[10] complex,[10a] and the $(C_5Me_4R)_2Zr(E)(NC_5H_5)$ complexes[10c] (E = O, S, Se, Te) were reported as well as the synthesis of zirconocene thioaldehyde complexes.[11] To our knowledge aliphatic thiolate complexes of Zr are virtually unknown, and only a brief report on the synthesis of the blue $Zr(SPh)_4$ complex has appeared in the literature.[12]

In the past we have reported briefly[13,14] on the synthesis and structural characterization of the $Zr_3S_3(^tBuS)_2(BH_4)_4(THF)_2$,

® Abstract published in *Advance ACS Abstracts*, July 1, 1994.

(1) (a) Coucouvanis, D.; Hadjikyriacou, A.; Toupadakis, A.; Koo, S. M.; Ileperuma, O.; Draganjac, M.; Salifoglou, A. *Inorg. Chem.* **1991**, *30*, 754–767. (b) Halbert, T. R.; Pan, W.-H.; Stiefel, E. I. *J. Am. Chem. Soc.* **1983**, *105*, 5476. (c) Coucouvanis, D.; Toupadakis, A.; Koo, Sang-Man; Hadjikyriacou, A. I. *Polyhedron* **1989**, *8*, 1705. (d) Draganjac, M.; Rauchfuss, T. B. *Angew. Chem., Int. Ed. Engl.*, **1985**, *24*, 742.
(2) (a) Coucouvanis, D.; Draganjac, M. E.; Koo, S. M.; Toupadakis, A.; Hadjikyriacou, A. I. *Inorg. Chem.* **1992**, *31*, 1186–1196. (b) Coucouvanis, D.; Draganjac, M. *J. Am. Chem. Soc.* **1982**, *104*, 6820.
(3) (a) Kim, C. G.; Coucouvanis, D. *Inorg. Chem.* **1993**, *32*, 1881. (b) Kim, C. G.; Coucouvanis, D. *Inorg. Chem.* **1993**, *32*, 2232.
(4) (a) Rappe, A. K.; Goddard, W. A., III. *J. Am. Chem. Soc.* **1980**, *102*, 5115–5117. (b) Rappe, A. K.; Goddard, W. A., III. *J. Am. Chem. Soc.* **1982**, *104*, 448–456.
(5) Wolczanski, P. T.; Bercaw, J. E. *Acc. Chem. Res.* **1980**, *13*, 121.
(6) (a) Bennett, M. J.; Cowie, M.; Martin, J. L.; Takats, J. *J. Am. Chem. Soc.* **1973**, *95*, 7504. (b) Martin, J. L.; Takats, J. *Inorg. Chem.* **1974**, *13*, 73.
(7) (a) Bradley, D. C.; Gitlitz, M. H. *J. Chem. Soc. A* **1969**, 1152. (b) Muetterties, E. L. *Inorg. Chem.* **1974**, *13*, 1011.
(8) Bruder, A. H.; Fay, R. C.; Lewis, D. F.; Sayler, A. *J. Am. Chem. Soc.* **1976**, *98*, 6932.
(9) Kovacs, J. A.; Bergman, R. G. *J. Am. Chem. Soc.* **1989**, *111*, 1131–1133.
(10) (a) Hey, E.; Lappert, M. F.; Atwood, J. L.; Bott, S. G. *J. Chem. Soc., Chem. Commun.* **1987**, 421. (b) Bottomley, F.; Drummond, D. F.; Egharevba, G. O.; White, P. S. *Organometallics*, **1986**, *5*, 1620. (c) Howard, W. A.; Parkin, G. *J. Am. Chem. Soc.* **1994**, *116*, 606–615.
(11) Buchwald, S. J.; Nielsen, R. B. *J. Am. Chem. Soc.* **1988**, *110*, 3171–3175.
(12) Funk, H.; Hesselbarth, M. *Z. Z. Chem.* **1966**, *6*, 227.
(13) Coucouvanis, D.; Lester, R. K.; Kanatzidis, M. G.; Kessissoglou, D. P. *J. Am. Chem. Soc.* **1985**, *107*, 8279.
(14) Coucouvanis, D.; Hadjikyriacou, A.; Kanatzidis, M. G. *J. Chem. Soc., Chem. Commun.* **1985**, 1224.

0020-1669/94/1333-3645$04.50/0

I, $Zr_6S_6(^tBuS)_4(BH_4)_8(THF)_2$, **II**, and $Zr_3(S)(^tBuS)_{10}$, **III**, aggregates[15] as the first examples of polynuclear Zr clusters that contain aliphatic thiolate and sulfide ligands. A common structural motif in these compounds is a hexagonal bipyramidal Zr_3S_5 unit that contains puckered $Zr_3(\mu_2\text{-}SR)_{3-n}(\mu\text{-}S)_n$ equatorial planes and μ_3-S or μ_3-SR axial ligands. The μ-sulfido ligands in these clusters were not externally supplied and were generated *in situ* as a result of aliphatic C–S bond cleavage. In this paper we report on the detailed syntheses and structures of **I–III** and also on a new anionic dimeric complex, $(Mg(THF)_6)[Zr_2(SPh)_{7.2}(CH_2Ph)_{1.8}]_2\cdot 3THF$, **IV**, that is obtained in a reaction that employs benzenethiolate ligands. In the latter the robust phenyl C–S bonds do not undergo cleavage reactions, and as the structure of **IV** indicates, the central dimeric unit is supported by three μ_2-SPh ligands. After we initiated the studies reported in this paper, Bergman and co-workers showed that like the $(Cp^*)_2Zr{=}NR$[16] and $(Cp^*)_2Zr{=}O$[17] complexes, the $(Cp^*)_2Zr{=}S$ complex[18] also could be generated *in situ* and the existence of the Zr=S functional group was demonstrated in trapping experiments with alkynes, nitriles, or dative ligands. These reactions gave metallacycle derivatives following addition across the Zr=S bond or $(Cp^*)_2Zr(S)(L)$ derivatives (L = pyridines) by addition of ligands to the Zr atom and maintaining the Zr=S chromophore intact.

Experimental Section

General Procedures and Techniques. The reagents and solvents in this work were used as purchased, unless otherwise stated. All operations were performed *in the strict absence of moisture* under a dinitrogen atmosphere, using any of the following: (a) a high-vacuum line equipped with a diffusion pump; (b) a Schlenk line and cannulae and syringe techniques; (c) a Vacuum Atmospheres Dri-Lab glovebox. Acetonitrile (CH_3CN) and dichloromethane (CH_2Cl_2) were distilled over calcium hydride. Tetrahydrofuran (THF) and diethyl ether were distilled from Na/benzophenone ketyl radical solutions. Toluene and hexanes were distilled over fresh CaH_2 and redistilled from Na/K alloy (1:3) prior to use. Published procedures were followed for the syntheses of the $Zr(BH_4)_4$[19] and $Zr(CH_2Ph)_4$[20] complexes. The synthesis of $Zr_3S_3(^tBuS)_2(BH_4)_4(THF)_2$ and $Zr_3(S)(^tBuS)_{10}$ can be carried out via standard Schlenk techniques, but the yield loss is significant as a result of hydrolysis. The synthesis of $(Mg(THF)_6)[Zr_2(SPh)_{7.2}(CH_2Ph)_{1.8}]_2\cdot 3THF$ is particularly moisture sensitive, and the use of a high-vacuum line is necessary. For this synthesis both the solvent and the thiol were transferred into the reaction flask via vacuum distillation.

Elemental analyses were performed by Oneida Research Services, Inc., and Galbraith Analytical Laboratories, as well as by the analytical services laboratory in the department of chemistry at The University of Michigan.

Physical Methods. Infrared spectra were recorded on a Nicolet 60-SX FT-IR spectrometer or a Perkin-Elmer 1330 grating infrared spectrophotometer at a resolution of 4 cm^{-1} in KBr disks. Proton NMR spectra were obtained on a Bruker 360 MHz Fourier-transform (FT) NMR spectrometer with a superconducting magnet. Tetramethylsilane $(CH_3)_4Si$ was used as an internal standard. A Debye–Scherrer camera with nickel-filtered copper radiation was utilized to obtain X-ray powder diffraction patterns.

Synthesis. $Zr_3S_3(^tBuS)_2(BH_4)_4(THF)_2$, I. A quantity of $Zr(CH_4)_4$[19] (4.80 g, 32 mmol) was sublimed in vacuum, using liquid nitrogen, into a three-necked 250-mL round-bottomed flask equipped with a stirring bar and fitted with a stopcock, rubber septum, and a reflux condenser. To this flask was added 80 mL of THF to dissolve the solid, and then 15.5 mL of ^{t}BuSH (140 mmol) was added and the solution stirred under dry dinitrogen for 30 min. Gas evolved steadily (H_2) as the solution became pale yellow. The solution was then heated to *ca.* 50 °C for an additional 4–6 h. At this stage the volume of the solvent was reduced in vacuum to ca. 30 mL and an equal volume of diethyl ether was added. To this solution *n*-hexane was slowly added to incipient crystallization, and the mixture was stored at –20 °C overnight. The yellow microcrystalline solid was filtered out, washed with hexane, and vacuum dried. The yield was 5.8 g, 7.7 mmol (73%) based on the $Zr(BH_4)_4$ used. The solid is exceedingly moisture sensitive and turns white upon exposure to even imperceptible amounts of moisture.

Anal. Calcd for $Zr_3S_5O_2C_{16}B_4H_{50}$: C, 25.66; H, 6.68; B, 5.88; S, 21.39; Zr, 36.09. Found: C, 26.69; H, 7.31; B, 5.87; S, 19.10; Zr, 35.33. FT-IR (KBr pellet, cm^{-1}): $\nu(B\text{–}H_t)$, 2527 (s), 2465(s), 2414(s); $\nu(B\text{–}H_b)$, 2182 (s), 2111 (s), 2050 (sh), 1986 (s); $\nu(Zr\text{–}H\text{–}B)$, 1232 (vs); $\nu(C\text{–}S)$ (838 (vs). X-ray powder pattern spacings (Å): 12.00 (s), 9.25 (s), 8.30 (vs), 7.50 (m), 7.00 (vw), 6.85 (vw), 6.65 (m), 5.8 (w), 5.5 (w), 5.2 (w), 4.8 (m), 4.4 (w), 4.15 (w), 4.00 (vw), 3.80 (vw), 3.7 (m), 3.5 (w), 3.3 (vw), 3.2 (vw), 2.95 (m).

$[BH_2(^tBuS)]_3$. The pale yellow filtrate that was obtained following the isolation of **I** was taken to dryness under vacuum. The solid that remained was extracted with *n*-hexane. The hexane solution was filtered, and the filtrate was concentrated in vacuum to near dryness. The yellow microcrystalline solid that formed was isolated. The yield was 7.5 g. Anal. Calcd for SC_4BH_{11}: C, 47.10; H, 10.89; B, 10.60; S, 31.43. Found: C, 46.38; H, 10.28; B, 8.75; S, 29.94. FT-IR (KBr pellet, cm^{-1}): $\nu(B\text{-}H_t)$, 2420 (vs), 2470 (sh). X-ray powder pattern spacings (Å): 14.00 (vw), 10.50 (w), 8.75 (w), 7.75 (s), 6.95 (s), 6.40 (m), 6.00 (m), 5.60 (m), 5.0 (vs), 4.60 (s), 3.9 (m), 3.7 (m), 3.55 (w), 3.45 (w), 3.25 (vw), 2.98 (w).

$Zr_6S_6(^tBuS)_4(BH_4)_8(THF)_2$, II. A sample of $Zr_3S_3(t\text{-}C_4H_9S)_2(BH_4)_4(THF)_2$, **I**, was dissolved in 5 mL of CD_2Cl_2 to give a concentrated pale yellow solution for use in ^{1}H-NMR spectroscopic studies. The solution was filtered and was stored at ambient temperature for 1 day. In this period it slowly deposited a flocculent solid and a few small pale yellow crystals. One of these crystals was used in the X-ray crystal structure determination. Unfortunately the remaining sample decomposed and no analytical or spectroscopic data could be obtained for the compound. Repeated attempts to grow these crystals as indicated above have failed, and only noncrystalline intractable solids could be obtained.

$Zr_3(^tBuS)_{10}(S)$, III. A quantity of $Zr(CH_2Ph)_4$[20] (9.00 g, 19.77 mmol) was dissolved in ca. 200 mL of dry toluene. To this solution was added 8.92 mL of ^{t}BuSH (79.0 mmol), and the mixture was stirred overnight at ambient temperature. The solvent was removed by vacuum distillation, and the orange powder that remained was recrystallized from a saturated diethyl ether solution by cooling to –20 °C. The yield was 6.1 g of yellow needles or 75% based on $Zr(CH_2Ph)_4$. The 360-MHz NMR spectrum of the recrystallized product was very clean and showed four resonances at 1.81, 1.93, 2.01, and 2.32 ppm with an intensity ratio of 3:3:3:1. The NMR spectrum is entirely consistent with the solid-state molecular structure as determined by X-ray crystallography.

The reaction was also carried out in hexane, and a gas chromatographic/mass spectrometric analysis of the reaction volatile species was undertaken after the reaction was complete. In addition to the components that were present in the solvent (various hexane and hexene isomers), two new peaks were clearly seen in the chromatogram and were identified on the basis of their fragmentation patterns. The one with the shortest retention time was identified as isobutene, and the second was toluene. Integration of the areas isobutene:toluene gave a ratio close to 1:60. This integration is not quantitatively accurate and reflects problems associated with the detection of the alkene that, relative to toluene, is produced in small amount in this reaction.

$(Mg(THF)_6)[Zr_2(SPh)_{7.2}(CH_2Ph)_{1.8}]_2\cdot 3THF$, IV. A few crystals of **IV** originally were obtained when $Zr(CH_2Ph)_4$ contaminated with $PhCH_2MgCl$ was inadvertedly used in the synthesis.[20] Our unsuccessful attempts to obtain crystals with any of a number of other counterions led to the intentional use of the $CH_2PhMgCl$ molecule as a source of the apparently important $(Mg(THF)_6)^{2+}$ cation.

A mixture of $Zr(CH_2Ph)_4$ and $PhCH_2MgCl$ in a 2:1 molar ratio (2.0 g) was suspended in 50 mL of THF, and 1.80 mL of PhSH was added at –78 °C. The reaction vessel was allowed to stand in the cold bath overnight and attained ambient temperature after ca. 16 h. Upon warming, the reaction slowly took place to give a saturated solution of the compound that precipitated out of solution in crystalline form. The yield was 1.4 g. Anal. Calcd for $(Mg(THF)_6)[Zr_2(SPh)_{7.2}(SPh)_{7.2}$-

(15) Abbreviations used in this paper: ^{t}BuSH = tertiary butanethiol, C_4H_9SH; $(CH_2Ph)^-$ = the benzyl anion, $C_7H_7^-$; THF = tetrahydrofuran, C_4H_4O.

(16) Walsh, P. J.; Hollander, F. J.; Bergman, R. G. *J. Am. Chem. Soc.* **1988**, *110*, 8729–31.
(17) Carney, M. J.; Walsh, P. J.; Hollander, F. J.; Bergman, R. G. *J. Am. Chem. Soc.* **1989**, *111*, 8751–53.
(18) Carney, M. J.; Walsh, P. J.; Bergman, R. G. *J. Am. Chem. Soc.* **1990**, *112*, 6426–28.
(19) James, B. D.; Nanda, R. K.; Wallbridge, M. G. H. *J. Chem. Soc.* **1966**, A182.
(20) Zucchini, V.; Albizzati, E.; Giannini, V. *J. Organomet. Chem.* **1971**, *26*, 357. The $CH_2PhMgCl$ Grignard reagent is used in the synthesis of the $Zr(CH_2Ph)_4$ complex from $ZrCl_4$.

Table 1. Summary of Crystal Data, Intensity Collection, and Structure Refinement of $Zr_3S_3(^tBuS)_2(BH_4)_4(THF)_2$, I, $Zr_6S_6(^tBuS)_4(BH_4)_8(THF)_2{\cdot}2CH_2Et_2O$, II, $Zr_3(S)(^tBuS)_{10}$, III, and $(Mg(THF)_6)[Zr_2(SPh)_{7.2}(CH_2Ph)_{1.8}]_2{\cdot}3THF$, IV

	I	II	III	IV
formula	$Zr_3S_5O_2C_{16}B_4H_{50}$	$Zr_6Cl_4S_{10}O_2C_{26}B_8H_{88}$	$Zr_3S_{11}O_{0.5}C_{42}H_{95}$	$Zr_4S_{14.4}MgO_9C_{147.6}H_{169.2}$
MW	751.8	1529.16	1234.6	2931
a, Å	11.545(3)	12.443(1)	22.009(8)	14.352(6)
b, Å	16.481(4)	15.197(2)	11.372(4)(6)	22.307(14)
c, Å	18.118(4)	18.365(2)	26.980(7)	23.554(8)
α, deg	90.00	90.00	90.00	90.00
β, deg	91.23(2)	70.214(7)	101.93(3)	95.46(3)
γ, deg	90.00	90.00	90.00	90.00
V, Å^3; Z	3447(1); 4	3267.5(5); 2	6607(4); 4	7506; 2
d_{calc},[a] g/cm^3	1.45	1.55	1.24	1.30
space group	$P2_1/c$	$P2_1/c$	$P2_1/c$	$P2_1/c$
cryst dimens, mm	0.08 × 0.34 × 0.26	0.21 × 0.135 × 0.205		0.3 × 0.4 × 0.6
μ, cm^{-1}	11.4	12.5	8.15	4.8
radiation	Mo Kα1[b]	Mo Kα1[b]	Mo Kα1[b]	Mo Kα1[b]
data collect	$2\theta_{max}$ = 40°	$2\theta_{max}$ = 45°	$2\theta_{max}$ = 40°	$2\theta_{max}$ = 34°
no. of data used ($F_o^2 > 3\sigma(F_o^2)$)	2169	3102	3966	2582[c]
no. of params	235	278	315	387
R_d[d]	0.051	0.042	0.072	0.075
R_w[e]	0.050	0.043	0.069	0.070

[a] The extreme sensitivity of these complexes to moisture and oxygen precluded a meaningful determination of their densities. [b] λ = 0.709 26 Å. [c] $F_o^2 > 3\sigma(F_o^2)$. [d] $R = \sum||F_o| - |F_c||/|F_o|$. [e] $R_w = [\sum w(|F_o| - |F_c|)^2/\sum w|F_o|^2]^{1/2}$.

$(CH_2Ph)_{1.8}]_2{\cdot}3THF$: C, 60.59; H, 5.80; S, 15.28; Mg, 0.83, Zr, 12.45. Calcd for $(Mg(THF)_6)]Zr_2(SPh)_9]_2{\cdot}3THF$: C, 58.32; H, 4.25; S, 19.44; Mg, 0.82; Zr, 12.31. Found: C, 56.61; H, 5.45; S, 18.19; Mg, 0.86; Zr, 16.44. The extreme sensitivity of this compound toward hydrolysis obviously precludes an accurate elemental analysis. Nevertheless, the available analytical data (with the exception of the Zr analysis that maybe incorrect) suggest that the bulk of the compound may be a mixture of isomorphous crystals of the type $(Mg(THF)_6)[Zr_2(SPh)_{9-x}(CH_2Ph)_x]_2{\cdot}3THF$ (x = 0–2).

X-ray Diffraction Measurements. (a) Collection of Data. Single crystals of **I** were obtained from saturated THF solutions upon addition of diethyl ether and *n*-hexane and cooling to –20 °C. A concentrated solution of **I** in CD_2Cl_2 upon standing for ca. 24 h at ambient temperature deposited yellow crystals of **II** with a powder diffraction pattern different from that of **I**. Orange single crystals of **III** were obtained by cooling saturated diethyl ether solutions of **III**. Crystals of **IV** suitable for X-ray measurements were obtained by cooling saturated THF solutions of **IV**.

A single crystal for each complex was carefully chosen and mounted in a thin-walled, sealed capillary tube. Diffraction data for **I–IV** were collected on a Nicolet P3/F four-circle, computer-controlled diffractometer at ambient temperature, and also a second data set was collected at –50 °C for **IV**. Graphite-monochromatized Mo Kα radiation ($2\theta_m$ = 12.50°) was used for data collection and cell dimension measurements (Kα, λ = 0.7107 Å).

Intensity data for all crystals were obtained using a θ–2θ step scan technique. Throughout the data collection three standard reflections were monitored every 100 reflections to determine crystal and instrumental stability. No crystal decay was observed for **I–III**. For **IV** a significant crystal decay was observed for the data collected at ambient temperature. The mean drop of intensity was 13.5% with a maximum drop of 25%. A correction curve based on the standards was used to correct for this crystal decay. No crystal decay was observed when data were obtained at the lower temperature. Accurate cell parameters were obtained from a least squares fit of the angular settings, (2θ, ω, ϕ, χ), of 25 machine-centered reflections with 2θ values between 10 and 30°. Details concerning crystal characteristics and X-ray diffraction methodology are shown in Table 1. The raw data obtained were reduced according to a protocol described earlier.[21]

Due to the small μ values (Table I), and the small size of the crystals, no absorption corrections were applied to any of the data sets.

(b) Determination of Structures. $Zr_3S_3(^tBuS)_2(BH_4)_4(THF)_2$, I. The structure was solved with the direct methods routine SOLV of the SHELXTL 84 package of crystallographic programs. The three Zr atoms were located first, and their positions were verified with a sharpened Patterson synthesis map. Subsequent Fourier syntheses and electron density maps revealed the locations of the remaining sulfur, carbon, boron, and oxygen atoms. Isotropic refinement converged to an R value of 0.09. At this stage positional disorder was detected for the THF ligand attached to Zr(1). One carbon atom (C(16)) attached to O(1) was found to occupy two different sites above and below the approximate O(1)C(13)C(14)C(15) THF plane. After numerous cycles of refinement with isotropic temperature factors assigned to all nondisordered, non-hydrogen atoms the refinement converged to a final R value of 0.061. At this stage the hydrogen atoms were included in the structure factor calculations at their calculated positions but were not refined. At convergence, with all atoms in the asymmetric unit present, the final R values were 0.05 and 0.05 for R and R_w, respectively. The last shift/esd was less than 0.002.

$Zr_6S_6(^tBuS)_4(BH_4)_8(THF)_2$, II. The structure was solved with the direct methods routine SOLV of the SHELXTL 84 package of crystallographic programs. The hexanuclear cluster is required by space group considerations to reside on a crystallographic inversion center at $0, {}^1/_2, 0$. The three Zr atoms were located first, and their positions were verified with a sharpened Patterson synthesis map. Subsequent Fourier syntheses revealed the locations of the remaining non-hydrogen atoms. The atomic positions were refined with isotropic temperature factors to an R value of 0.12. At this stage a difference Fourier map revealed the presence of a disordered CH_2Cl_2 molecule. The nature of the disorder appears to be 3-fold with the solvent molecule occupying the site in three orientations with roughly equal occupancy factors.

Anisotropic refinement (two cycles) of all nondisordered atoms gave an R value of 0.067. At this point the Fourier difference map revealed that the THF ligand also was positionally disordered and was found equally distributed in three positions rotated relative to each other around the Zr–O bond. All of the carbon atoms of the disordered THF molecule were refined with isotropic temperature factors. The C–Cl distances of the disordered CH_2Cl_2 molecule of solvation were fixed to 1.65 Å due to anomalous, erratic behavior in the refinement process.

The positions of the *tert*-butyl hydrogen atoms as well as the BH_4 terminal H atoms were calculated, and the H atoms were included in the structure factor calculation but were not refined. Refinement of this model by full-matrix least squares methods converged to final values of R = 0.044 and R_w = 0.044.

$Zr_3(S)(^tBuS)_{10}$, III. The coordinates of the three zirconium atoms were obtained from direct methods (SHELX-76 crystallographic package) in the space group $P2_1/c$ with Zr–Zr separations at 3.6 Å. All non-hydrogen atoms were located via successive difference electron density maps using 2θ = 30° diffraction data. Isotropic refinement of the structure gave an R value of 13.4%. A second set of reflections (2θ = 30–40°) was obtained and was merged with the 30° set. Isotropic refinement was continued using reflections with $I > 3\sigma(I)$ to an R value of 12.3%. Anisotropic refinement of the zirconium atoms gave R = 11.4%. At this stage it became apparent that sulfur S(1) was disordered. A site occupancy factor of 0.7 was assigned to S(1), and its alternative S(1X) was refined with a 0.3 occupancy factor. Finally the hydrogen atoms were included in the structure factor calculation but they were not refined. The final R value was 0.069.

$(Mg(THF)_6)[Zr_2(SPh)_{7.2}(CH_2Ph)_{1.8}]_2{\cdot}3THF$, IV. From diffraction data obtained at ambient temperature, ~298 K, a Patterson map was

(21) Al-Ahmad, S. A.; Salifoglou, A.; Kanatzidis, M. G.; Dunham, W. R.; Coucouvanis, D. *Inorg. Chem.* **1990**, *29*, 927.

Table 2. Fractional Atomic Coordinates and Isotropic Temperature Factors[a] for $Zr_3S_3(t\text{-}C_4H_9S)_2(BH_4)_4(THF)_2$, **I**

atom	x	y	z	U
Zr(1)	0.4019(01)	0.4735(01)	0.2643(01)	0.0486
Zr(2)	0.3190(01)	0.5939(01)	0.3970(01)	0.0468
Zr(3)	0.1427(01)	0.5867(01)	0.2326(01)	0.0426
S(1)	0.3602(04)	0.6256(02)	0.2616(02)	0.0467
S(2)	0.2005(03)	0.4791(02)	0.3280(02)	0.0443
S(3)	0.4727(04)	0.4921(03)	0.3916(02)	0.0636
S(4)	0.2377(03)	0.4659(02)	0.1604(02)	0.0461
S(5)	0.1089(04)	0.6502(02)	0.3636(02)	0.0481
B(1)	0.5724(17)	0.4622(13)	0.1961(12)	0.0684
B(2)	0.4090(20)	0.7010(13)	0.4618(11)	0.0751
B(3)	−0.0497(17)	0.5635(13)	0.1970(10)	0.0649
B(4)	0.1589(21)	0.7098(12)	0.1505(10)	0.0754
O(1)	0.2444(10)	0.5386(07)	0.4985(05)	0.0671
O(2)	0.3828(11)	0.3395(06)	0.2804(06)	0.0741
C(1)	0.2768(16)	0.4821(11)	0.0601(08)	0.0599
C(2)	0.3274(17)	0.3990(12)	0.0358(09)	0.0884
C(3)	0.1613(17)	0.4985(12)	0.0192(08)	0.0817
C(4)	0.3640(17)	0.5503(12)	0.0503(09)	0.0838
C(5)	0.0769(16)	0.7598(11)	0.3703(09)	0.0655
C(6)	0.1736(20)	0.8146(10)	0.3460(11)	0.0936
C(7)	0.0536(19)	0.7774(12)	0.4499(10)	0.1067
C(8)	−0.0268(17)	0.7773(11)	0.3231(11)	0.0931
C(9)	0.2343(16)	0.4522(12)	0.5166(10)	0.0293
C(10)	0.1949(20)	0.4517(14)	0.5979(12)	0.0402
C(11)	0.1507(21)	0.5282(16)	0.6138(13)	0.0449
C(12)	0.1875(21)	0.5870(15)	0.5563(14)	0.0434
C(13)	0.3749(24)	0.2831(19)	0.2273(15)	0.0527
C(14)	0.3349(21)	0.2004(16)	0.2602(14)	0.0458
C(15)	0.3637(22)	0.2174(16)	0.3363(14)	0.0476
C(16)	0.4429(43)	0.2965(30)	0.3449(26)	0.0417
C(16′)	0.3196(39)	0.2997(27)	0.3509(24)	0.0352

[a] Equivalent isotropic temperature factor U_{eq} (Å^2) defined as one-third of the trace of the orthogonalized U_{ij} tensor.

calculated (SHELX-86 crystallographic package) and was solved to reveal the positions of the two zirconium atoms. Seven thiophenolate and two benzyl ligands were located in successive difference Fourier electron density maps. The four dimeric monoanions are located on general positions in the space group $P2_1/c$, and the two dipositive $[Mg(THF)_6]^{2+}$ cations are located on centers of symmetry at $^1/_2$, $^1/_2$, 0 and $^1/_2$, 0, $^1/_2$. In the asymmetric unit there is one THF molecule of solvation. An additional, ill-behaving molecule of THF also was located on a general position with half-occupancy and was refined with fixed positional parameters. One of the two benzyl ligand sites is occupied by both a benzyl ligand at 80% occupancy and a benzenethiolate ligand at 20% occupancy. Consequently CBI consists of 80% carbon and 20% S. Isotropic refinement converged to an R value of 9.4%. The two zirconium atoms, the magnesium atom, and five sulfur atoms were refined with anisotropic temperature parameters to keep the data/parameter ratio at 6.7. The positions of the hydrogen atoms were calculated and included in the structure but were not refined. Final R values: $R = 0.087$ and $R_w = 0.081$. The structure also was refined using the low-temperature diffraction data. Both THF solvate molecules were ordered and refined without constraints placed on them. Isotropic refinement gave $R = 0.0750$ and $R_w = 0.069$, but no significant differences in the bond distances and angles were found.

(c) Crystallographic Results. The final atomic positional parameters for $Zr_3S_3(^tBuS)_2(BH_4)_4(THF)_2$, **I**, $Zr_6S_6(^tBuS)_4(BH_4)_8(THF)_2$, **II**, $Zr_3(S)(^tBuS)_{10}$, **III**, and $(Mg(THF)_6)[Zr_2(SPh)_{7.2}(CH_2Ph)_{1.8}]_2\cdot 3THF$, **IV**, with standard deviations can be found in Tables 2–5, respectively. Intramolecular distances and angles are given in Table 6. The numbering schemes for the anions in **I**–**IV** are shown in Figures 1–4, respectively.

Results and Discussion

Synthesis. The acidification of the Zr-bound BH_4^- and $(CH_2Ph)^-$ ligands in the $Zr(BH_4)_4$ and $Zr(CH_2Ph)_4$ complexes by RSH molecules has been found to be a convenient synthetic method for the introduction of sulfur ligands to the coordination sphere of Zr(IV). Concomitant with the generation of the thiolate anions, protonation of the BH_4^- and $(CH_2Ph)^-$ anions by RSH generates the diborane and toluene molecules, respectively. All of the polynuclear Zr clusters reported herein are exceedingly air-sensitive solids soluble in THF, CH_2Cl_2, benzene, and CH_3CN. The extreme difficulties in handling these compounds may account for the rather unsatisfactory elemental analyses obtained for some of them.

Table 3. Fractional Atomic Coordinates and Isotropic Temperature Factors[a] for $Zr_6S_6(t\text{-}C_4H_9S)_{(}BH_4)_8(THF)_2$, **II**

atom	x	y	z	U
Zr(1)	−0.0720(01)	0.4023(01)	−0.0230(00)	0.0364
Zr(2)	0.2137(01)	0.3504(01)	−0.1164(00)	0.0391
Zr(3)	0.0077(01)	0.2948(01)	−0.2000(00)	0.0416
S(1)	0.0716(02)	0.4412(01)	−0.1621(01)	0.0366
S(2)	0.0273(02)	0.2518(020	−0.0720(01)	0.0422
S(3)	0.1029(02)	0.4287(01)	0.0144(01)	0.0405
S(4)	−0.1761(02)	0.3825(02)	−0.1252(01)	0.0453
S(5)	0.2289(02)	0.2949(02)	−0.2568(01)	0.0458
O	0.0104(06)	0.3654(04)	−0.3109(03)	0.0643
C(1)	−0.3220(08)	0.3294(07)	−0.0978(06)	0.0604
C(2)	−0.4031(09)	0.3991(09)	−0.0485(07)	0.0802
C(3)	−0.3465(09)	0.3181(08)	−0.1738(06)	0.0810
C(4)	−0.3263(10)	0.2435(08)	−0.0576(07)	0.0875
C(5)	0.3095(09)	0.1903(07)	−0.2993(05)	0.0572
C(6)	0.2598(10)	0.1113(07)	−0.2515(07)	0.0791
C(7)	0.2971(11)	0.1821(09)	−0.3778(06)	0.0944
C(8)	0.4307(10)	0.2032(08)	−0.3043(07)	0.0793
B(1)	−0.2128(10)	0.3546(08)	0.0854(07)	0.0584
B(2)	0.2948(11)	0.2201(08)	−0.0683(06)	0.0644
B(3)	0.3779(09)	0.4363(08)	−0.1518(07)	0.0585
B(4)	−0.0623(15)	0.1694(08)	−0.2350(09)	0.0950
C(1A)	0.1140(37)	0.4131(29)	−0.3544(24)	0.0326
C(2A)	0.0587(37)	0.4299(30)	−0.4330(22)	0.0261
C(3A)	−0.0294(44)	0.4062(29)	−0.4222(24)	0.0251
C(4A)	−0.0845(31)	0.3700(25)	−0.3437(20)	0.0238
C(1B)	−0.0124(41)	0.4541(33)	−0.3176(27)	0.0355
C(2B)	−0.0189(26)	0.4666(18)	−0.3954(16)	0.0397
C(3B)	0.0651(27)	0.4818(21)	−0.4145(18)	0.0146
C(4B)	0.0389(39)	0.3363(29)	−0.3930(25)	0.0341
C(1C)	−0.0462(26)	0.3269(19)	−0.3648(16)	0.0147
C(2C)	−0.0829(35)	0.4146(27)	−0.3985(25)	0.0227
C(4C)	0.1000(17)	0.4536(89)	−0.3838(76)	0.0000
C(C1)	0.4751(01)	0.0536(71)	0.1333(66)	0.0717
Cl(1)	0.3907(27)	−0.0118(26)	−0.1402(22)	0.0694
Cl(2)	0.5904(44)	0.0395(28)	0.0880(27)	0.1082
C(C2)	0.4242(56)	0.0294(49)	0.1114(37)	0.0293
Cl(3)	0.4168(38)	−0.0653(23)	0.1685(22)	0.0989
Cl(4)	0.6070(35)	0.0631(24)	0.1333(22)	0.0621
C(C3)	0.5240(43)	−0.0242(33)	0.1240(29)	0.0335
Cl(5)	0.3724(43)	0.0204(34)	0.0712(32)	0.1531
Cl(6)	0.6531(30)	0.0787(24)	0.1045(26)	0.0810

[a] See footnote *a* in Table 2.

The type of oligonuclear Zr(IV) complexes that form in these reactions appears to depend on the nature of the thiol used and the ability of the C–S bond in the latter to undergo cleavage and generate the S^{2-} ligand. In the syntheses of **I** and **III**, the initial acid–base reactions are followed by C–S bond cleavage reactions within the Zr-coordinated $^tBuS^-$ ligands that generate the S^{2-} found in the final products. The absence of S^{2-} ligands in **IV** indicates that the C–S bonds in the PhS^- ligands do not undergo reductive cleavage. This observation may have important mechanistic implications regarding C–S bond cleavage in the Zr-coordinated thiolate ligands (vide infra).

The optimum conditions for the synthesis of the $Zr_3S_3(^tBuS)_2(BH_4)_4(THF)_2$ cluster, **I**, are reported in the Experimental Section. This reaction (eq 1) proceeds in THF at ambient temperature with a steady evolution of H_2 for about 30 min and goes to completion when the pale yellow solution is further heated to ~50 °C for 4–6 h. The same cluster, **I**, could be isolated in lower yields when the reaction was carried out without heating. Solutions of **I** in CH_2Cl_2, benzene, or CH_3CN are unstable and deposit intractable solids. After the isolation of **I** from solution, the very soluble $(BH_2{}^tBuS)_3$ byproduct also is obtained in 90% yield (based on eq 1) by evaporating solvent from filtrate to near dryness. The structure of this cyclic trimeric compound has been determined[22] (Figure 5). From the isolated yields of **I** and the

$(BH_2{}^tBuS)_3$ byproduct the overall stoichiometry of the reaction is best represented by eq 1.

$$3Zr(BH_4)_4 + 12{}^tBuSH + 2THF \rightarrow Zr_3S_3({}^tBuS)_2(BH_4)_4(THF)_2 + {}^7/_3(BH_2{}^tBuS)_3 + 15H_2 + 3C_4H_8 + {}^1/_2B_2H_6 \quad (1)$$

In the above equation the formation of H_2 was verified by NMR spectroscopy and the generation of C_4H_8, as a byproduct of the C–S bond cleavage in the $^tBuS^-$ ligand, is inferred and based on the positive identification of isobutene as one of the byproducts in the synthesis of **III** (vide infra). The 1,3,5-tri-*tert*-butyl)cyclotriborathiane (eq 1) undoubtedly forms as a result of a parallel reaction between unreacted thiol and the diborane generated in the acid–base, RSH/BH_4^-, reaction. The reactions of thiols with boranes were well-known,[23] and the mono(alkylthio)-borane products are obtained as polymers or trimers.[23,24] The independent synthesis of $(BH_2{}^tBuS)_3$ has been reported previously.[23]

In the early stages of the synthesis of **I**, and with a deficit of thiol, the formation of blue, monomeric paramagnetic Zr(III) complexes is apparent. One of these has been isolated and identified tentatively as the $Zr^{III}(BH_4)_2({}^tBuS)(THF)$ complex on the basis of marginal elemental analysis and a characteristic $S = {}^1/_2$ EPR spectrum. The detailed pathway that leads to the synthesis of **I** is not clear at this time; however, one of the possible routes to this molecule may be the condensation of coordinatively unsaturated Zr complexes that contain sulfido ligands. The identity of such complexes is difficult to ascertain although possible candidates may be suggested by an analysis of the structure of **I** in terms of viable fragments. An example of possible fragments and their condensation reaction is shown in eq 2.

$$2"[S{=}Zr^{IV}(BH_4)({}^tBuS)THF]" + "[S{=}Zr^{IV}(BH_4)_2THF]" \rightarrow Zr_3S_3({}^tBuS)_2(BH_4)_4(THF)_2 + THF \quad (2)$$

The availability of BH_4^- ligands in **I** prompted us to further explore the reactivity of these ligands with excess thiol. Attempts to obtain other clusters, in variations of reaction 1, employing longer reaction times (>12 h), a large excess of thiol at reflux temperature, or benzene as a solvent resulted in intractable solids that contained weak broad bands in the $B–H_{t,b}$ regions of the IR spectrum.

A concentrated solution of **I** in CD_2Cl_2 (prepared for ^{1}H-NMR measurements) upon standing for ca. 24 h at ambient temperature deposited yellow crystals of $Zr_6S_6({}^tBuS)_4(BH_4)_8(THF)_2$, **II**. The powder diffraction pattern of **II** was different than that of **I**. The single-crystal X-ray structures of **I** and **II** were determined[13] and reveal the trimeric nature of **I** and the hexameric nature of **II** (vide infra). We have been unable to reproduce the conditions that led to the original formation and crystallization of **II**. Nevertheless the fortuitous synthesis and the subsequent structural characterization of this cluster reveal a possible route for the transformation of **I** to intractable solids. The formation of **II** can be envisioned as the result of dissociation of a THF molecule from **I** followed by dimerization. A repetition of this process may lead to the Zr/S polymeric materials that form upon refluxing THF solutions of **I** and **II** or by dissolving these clusters in benzene (Figure 6).

The synthesis of **III** in toluene or hexanes occurs readily and for optimized conditions is described best by the following equation:

$$3Zr(CH_2Ph)_4 + 11{}^tBuSH \rightarrow Zr_3(S)({}^tBuS)_{10} + 11CH_3Ph + (CH_3)_2C{=}CH_2 \quad (3)$$

The toluene produced was quantitatively determined by ^{1}H-NMR spectroscopy; however, only a small amount of the expected isobutene was detected by a gas chromatographic/mass spectroscopic analysis, GC/MS (see Experimental Section).

The generation of the sulfido ligand found in **III** may involve either a heterolytic cleavage of the carbon–sulfur bond facilitated by the relative stability of the $^tBu^+$ carbonium ion (the latter may react with $^tBuS^-$ to give isobutene (Figure 7a) or a S-dealkylation reaction by a Lewis-base assisted β-proton elimination reaction (Figure 7b).

Qualitatively, the presence of ^{t}BuSH and isobutene detected in the reaction volatile products by GC/MS supports either of the two routes shown (Figure 7a,b). A carbonium ion mechanism has been proposed for the sulfur dealkylation of the mono-(thiolato)tungsten(IV) chlorides (eq 4).[25] In this case the isomer-

$$WCl_6 + Me_3SiS{}^iBu \rightarrow \{WCl_5(S{}^iBu)\} \rightarrow WS(Cl)_4 + {}^tBuCl \quad (4)$$

ization of the isobutyl group to *tert*-butyl provides convincing indirect evidence for the formation of a carbonium ion. In the synthesis of **III** no Zr(III) complexes have been detected in any stage of the reaction.

The ^{1}H NMR spectrum of **III** in benzene-d_6 shows four very sharp resonances in a 3:3:3:1 ratio at 1.81, 1.93, 2.01, and 2.32 ppm. These resonances reveal four different types of ^{t}Bu groups and indicate that the structure of **III** in solution is the same as that in the solid state (vide infra) and that the $^tBuS^-$ ligands do not undergo exchange.

The optimized synthesis of **IV** could be described by eq 5 on the basis of the quantitative appearance of toluene and the

$$4Zr(CH_2Ph)_4 + 2PhCH_2MgCl + 14PhSH + 6THF \rightarrow (Mg(THF)_6[Zr_2(SPh)_7(CH_2Ph)_2]_2 + MgCl_2 + 14CH_3Ph \quad (5)$$

composition of **IV**. The $PhCH_2MgCl$ in this reaction (chosen serendipitously; see Experimental Section) serves as a base but most importantly generates the $Mg(THF)_6^{2+}$ cation that makes it possible to obtain **IV** in crystalline form. The $Mg(THF)_6^{2+}$ counterion has been encountered previously in the $(Mg(THF)_6)$-$(ZrCl_6)$ salt.[26]

The lack of S^{2-} ligands in **IV** demonstrates the difficulty in breaking the C–S bond in the Zr-bound aromatic thiolate ligands. This may well derive from the inherent instability of the aromatic carbonium ions that would be involved in heterolytic bond cleavage reactions.

Description of Structures. The structures of **I–III** (Figures 1–3) are closely related and contain the distorted hexagonal bipyramidal core $[Zr_3(\mu_3\text{-}S)_2(\mu_2\text{-}S)_3]^{n+}$ as a structural feature. In **I** and **II** the Zr_3 subunits ($n = 4$) show two μ_2-$^tBuS^-$ ligands and a μ_2-S^{2-} ligand bridging the Zr atoms in the equatorial plane and two μ_3-S^{2-} ligands serving as "capping" ligands on the axial positions. In **III** ($n = 6$) three μ_2-$^tBuS^-$ ligands bridge the Zr atoms in the equatorial plane and μ_3-S^{2-} and μ_3-$^tBuS^-$ ligands serve as "caps" in the axial positions. The overall structure of **III** has a precedent in the crystallographically determined

(22) Kanatzidis, M. G.; Lester, R. K.; Kessissoglou, D.; Coucouvanis, D. *Acta Crystallogr.* **1987**, *C43*, 2148.
(23) Michailov, B. M. In *Progress in Boron Chemistry*; Brotherson, R. J., Steinberg, H. S., Eds.; Pergamon Press: Oxford, U.K.; Vol. 3.
(24) Muetterties, E. L.; Miller, N. E.; Packer, K. J.; Miller, H. C. *Inorg. Chem.* **1964**, *3*, 870.
(25) (a) Boorman, P. M.; O'Dell, B. D. *J. Chem. Soc., Dalton Trans.* **1980**, 257. *Inorg. Chim. Acta* **1976**, *19*, 135. (b) Boorman, P. M.; Chiveri, T.; Mahadev, K. N.; O'Dell, B. D. *Inorg. Chim. Acta* **1976**, *19*, 135.
(26) Sobota, P.; Utko, J.; Janas, Z. *J. Organomet. Chem.* **1986**, *316*, 19.

Table 4. Fractional Atomic Coordinates and Isotropic Temperature Factors[a] for $Zr_3(t\text{-}C_4H_9S)_{10}(S)$. III

atom	x	y	z	U
Zr(1)	0.6807(01)	0.2248(02)	0.3720(01)	0.0212
Zr(2)	0.7033(01)	0.2391(02)	0.2388(01)	0.0268
Zr(3)	0.8395(01)	0.2553(02)	0.3460(01)	0.0285
S(1)	0.8216(03)	0.3001(07)	0.2465(03)	0.0257
S(X1)	0.8228(06)	0.1868(12)	0.2521(05)	0.0077
S(2)	0.7932(02)	0.1957(04)	0.4238(02)	0.0283
S(3)	0.6147(02)	0.1703(04)	0.2833(02)	0.0231
S(4)	0.7338(02)	0.3921(04)	0.3195(02)	0.0236
S(5)	0.7469(02)	0.1113(04)	0.3185(02)	0.0258
S(6)	0.6377(03)	0.4014(04)	0.4029(02)	0.0398
S(7)	0.6293(02)	0.0993(04)	0.4233(02)	0.0300
S(8)	0.6586(03)	0.4123(05)	0.1924(02)	0.0520
S(9)	0.6863(03)	0.1101(05)	0.1665(02)	0.0439
S(10)	0.9324(02)	0.1389(05)	0.3640(02)	0.0476
S(11)	0.8903(02)	0.4427(05)	0.3723(02)	0.0542
C(1)	0.8706(10)	0.2271(19)	0.2105(08)	0.0182
C(2)	0.8458(09)	0.2306(17)	0.1541(07)	0.0139
C(3)	0.8642(13)	0.0783(26)	0.2200(11)	0.0335
C(4)	0.9370(09)	0.2413(19)	0.2294(07)	0.0170
C(5)	0.8178(08)	0.2660(17)	0.4876(07)	0.0126
C(6)	0.8845(09)	0.2260(18)	0.5059(07)	0.0157
C(7)	0.7752(09)	0.2111(18)	0.5200(07)	0.0153
C(8)	0.8123(10)	0.3958(20)	0.4858(08)	0.0181
C(9)	0.5339(08)	0.2256(15)	0.2633(06)	0.0089
C(10)	0.4961(08)	0.1653(16)	0.2991(07)	0.0103
C(11)	0.5308(09)	0.3584(17)	0.2667(07)	0.0137
C(12)	0.5106(08)	0.1833(17)	0.2081(07)	0.0118
C(13)	0.7294(08)	0.5569(15)	0.3189(06)	0.0083
C(14)	0.7530(09)	0.6045(17)	0.3708(07)	0.0129
C(15)	0.6603(08)	0.5928(16)	0.3007(07)	0.0116
C(16)	0.7706(08)	1.5996(16)	0.2816(07)	0.0114
C(17)	0.5825(09)	0.4104(18)	0.4485(08)	0.0155
C(18)	0.5674(11)	0.5390(22)	0.4494(09)	0.0231
C(19)	0.5258(10)	0.3404(20)	0.4290(08)	0.0200
C(20)	0.6162(10)	0.3678(20)	0.4994(09)	0.0215
C(21)	0.6411(08)	−0.0590(15)	0.4203(07)	0.0090
C(22)	0.7083(11)	−0.0890(22)	0.4341(09)	0.0249
C(23)	0.6136(09)	−0.1089(18)	0.3688(07)	0.0154
C(24)	0.6094(11)	−0.1128(22)	0.4585(09)	0.0235
C(25)	0.6323(09)	0.4246(17)	0.1215(07)	0.0119
C(26)	0.6120(12)	0.5531(23)	0.1127(09)	0.0269
C(27)	0.5786(10)	0.3483(19)	0.1038(08)	0.0182
C(28)	0.6841(09)	0.3933(18)	0.0960(07)	0.0142
C(29)	0.6790(11)	−0.0510(20)	0.1696(09)	0.0171
C(30)	0.7144(28)	−0.0991(56)	0.2146(23)	0.0932
C(31)	0.6918(18)	−0.0969(37)	0.1221(15)	0.0540
C(32)	0.6145(40)	−0.0742(79)	0.1720(31)	0.1436
C(33)	0.9355(10)	−0.0219(18)	0.3768(08)	0.0154
C(34)	0.9883(16)	−0.0706(31)	0.3598(13)	0.0433
C(35)	0.8769(16)	−0.0807(31)	0.3696(13)	0.0429
C36	0.9529(22)	−0.0304(42)	0.4323(18)	0.0693
C(37)	0.9757(09)	0.4653(17)	0.3896(07)	0.0136
C(38)	1.0048(11)	0.4277(21)	0.3457(09)	0.0230
C(39)	0.9813(10)	0.5993(21)	0.3964(09)	0.0212
C(40)	1.0016(09)	0.4020(19)	0.4374(08)	0.0163
O(X1)	0.1414(18)	0.1832(36)	0.3730(16)	0.0367
C(X1)	0.1724(22)	0.2731(46)	0.4810(19)	0.0260
C(X3)	0.1504(22)	0.1726(45)	0.4659(18)	0.0234
C(X3)	0.1110(20)	0.1951(39)	0.2860(17)	0.0197
C(X4)	0.1417(23)	0.1244(45)	0.3286(20)	0.0253
C(X5)	0.1732(25)	0.1409(49)	0.4221(22)	0.0305

[a] See footnote *a* in Table 2.

structures of analogous oxo complexes of Mo(IV), $Mo_3O(^tBuCH_2O)_{10}$,[27] and U(IV), $U_3O(^tBuO)_{10}$.[28] Both of these clusters contain the M_3O_{11} core that has been described[28] as "three distorted octahedra sharing an edge while also being mutually cofacial". A M_3O_{11} core of essentially the same general structure is found with the $[Mo_3(\mu_3\text{-}X)(\mu_3\text{-}Y)(OAc)_6(H_2O)_3]^-$ complexes[29]

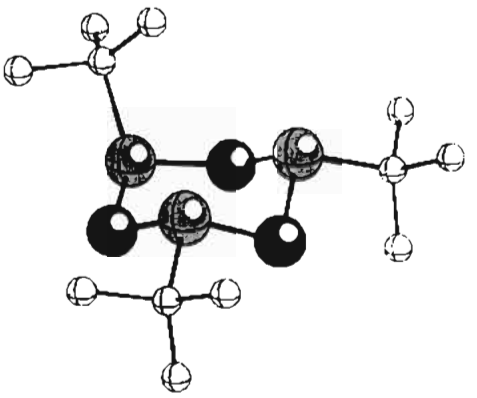

Figure 1. Structure of the $[BH_2{}^tBuS]_3$ cyclotriborathiane.[22]

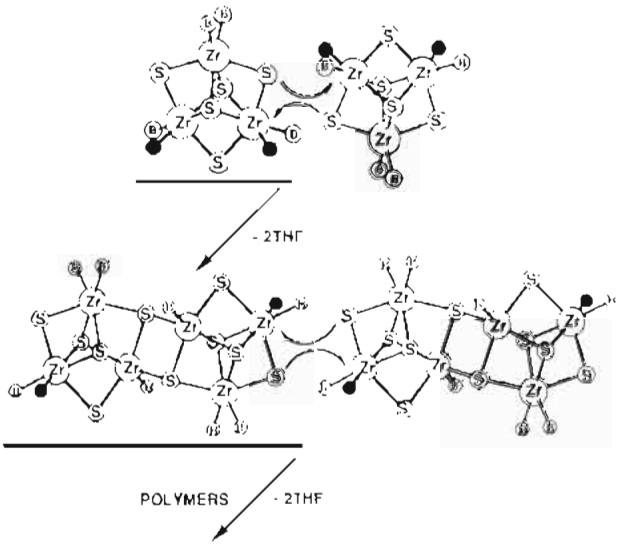

Figure 2. Proposed coupling reactions and oligomerization of the $[Zr_3(\mu_3\text{-}S)_2(\mu_2\text{-}S)_3]^{n+}$ Units in I and II.

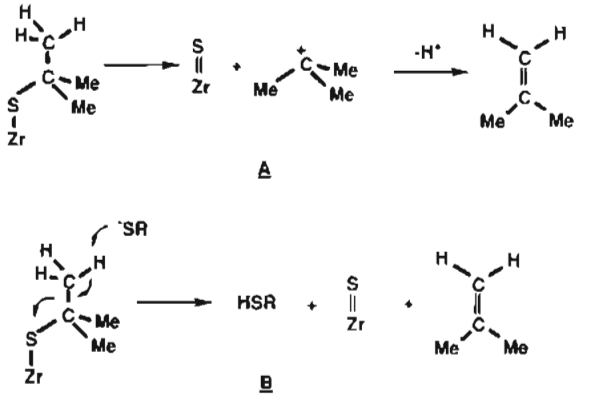

Figure 3. Proposed pathways for the C–S bond cleavage reaction in the Zr-coordinated, $^tBuS^-$ thiolate ligands.

(X = Y = O). In the latter six μ_2-acetate ligands and three terminal H_2O ligands complete the coordination spheres of the three octahedrally coordinated Mo(IV) ions.

The $[Zr_3(\mu_2\text{-}S)_2(\mu_2\text{-}S)_3]^{n+}$ core also can be described as the result of the cofacial fusion of three "octahedrally" coordinated Zr units (viewing the BH_4^- anions as monodentate ligands in **I** and **II**) and is quite close to an idealized hexagonal bipyramidal geometry (Table 7). The core structure of **II** (Figure 5) can be described in terms of two coupled Zr_3 cores identical to those found in **I**. The coupling can be visualized as the mutual displacement of a THF ligand in each of the two Zr_3 monomers, **I**, by the equatorial $\mu_2\text{-}S^{2-}$ ligand in the other. It should be noted that after coupling a BH_4^- ligand trans to the S^{2-} ligand has

(27) Chisholm, M. H.; Folting, K.; Huffman, J. C.; Kirkpatrick, C. C. *J. Am. Chem. Soc.* **1981**, *103*, 5967.
(28) Cotton, F. A.; Marler, D. O.; Schwotzer, W. *Inorg. Chim. Acta* **1984**, *95*, 207.
(29) Bino, A.; Cotton, F. A.; Dori, Z. *J. Am. Chem. Soc.* **1981**, *103*, 243.

Table 5. Fractional Atomic Coordinates and Isotropic Temperature Factors[a] for $Mg(THF)_6[Zr_2(SPH)_{7.2}(Bz)_{1.82}\cdot 3THF$, IV, at −50 °C

atom	x	y	z	U_{iso}	atom	x	y	z	U_{iso}
Zr(1)	0.2881(3)	0.7351(2)	0.6406(2)	0.030	C(31)	0.1116(37)	0.6384(16)	0.5493(15)	0.026
Zr(2)	0.1357(3)	0.6107(2)	0.7103(2)	0.030	C(32)	0.1924(31)	0.6332(18)	0.5271(17)	0.036
Mg(1)	0.5	0.5	0.0	0.032	C(33)	0.1814(35)	0.5846(20)	0.4743(20)	0.070
S(1)	0.3172(9)	0.8413(5)	0.6737(5)	0.070	C(34)	0.0832(37)	0.5694(16)	0.4549(16)	0.033
S(2)	0.2578(10)	0.7812(6)	0.5437(5)	0.083	C(35)	0.0049(36)	0.5889(21)	0.4822(23)	0.082
S(3)	0.4603(9)	0.7361(6)	0.6230(5)	0.082	C(36)	0.0121(36)	0.6241(20)	0.5328(19)	0.062
S(4)	0.3050(8)	0.6195(5)	0.6640(4)	0.037	C(37)	0.1934(26)	0.4737(16)	0.6461(17)	0.016
S(5)	0.2227(8)	0.7173(5)	0.7409(4)	0.027	C(38)	0.2096(32)	0.4833(19)	0.5892(20)	0.060
S(6)	0.1188(8)	0.6807(5)	0.6153(5)	0.041	C(39)	0.2852(33)	0.4468(20)	0.5717(17)	0.047
S(7)	0.0880(10)	0.5134(6)	0.6663(6)	0.087	C(40)	0.3375(31)	0.4068(19)	0.6082(21)	0.063
C(B1)	0.2376(22)	0.5675(13)	0.7847(12)	0.080	C(41)	0.3079(33)	0.4023(18)	0.6656(19)	0.056
C(B2)	0.1680(27)	0.5487(18)	0.8301(16)	0.026	C(42)	0.2328(34)	0.4358(20)	0.6885(19)	0.063
C(B3)	0.1280(30)	0.4893(19)	0.8267(16)	0.042	O(1)	0.5375(17)	0.4127(10)	0.0338(10)	0.035
C(B4)	0.0654(31)	0.4746(19)	0.8703(19)	0.060	C(T1)	0.5147(25)	0.3540(16)	0.0026(14)	0.018
C(B5)	0.0513(27)	0.5123(18)	0.9169(15)	0.025	C(T2)	0.5373(29)	0.3097(17)	0.0498(17)	0.045
C(B6)	0.0887(29)	0.5712(19)	0.9194(16)	0.037	C(T3)	0.6159(31)	0.3344(18)	0.0887(16)	0.049
C(B7)	0.1508(28)	0.5890(16)	0.8753(17)	0.032	C(T4)	0.5913(28)	0.4025(17)	0.0922(16)	0.038
C(B8)	0.0151(27)	0.6590(16)	0.7547(14)	0.030	O(2)	0.3632(17)	0.4914(11)	0.0321(10)	0.033
C(B9)	−0.0525(30)	0.6065(20)	0.7339(20)	0.051	C(T5)	0.3312(33)	0.4356(18)	0.0628(17)	0.056
C(B10)	−0.0772(30)	0.5607(21)	0.7713(17)	0.045	C(T6)	0.2257(37)	0.4512(22)	0.0729(19)	0.092
C(B11)	−0.1364(31)	0.5145(18)	0.7493(19)	0.047	C(T7)	0.2203(32)	0.5212(21)	0.0715(18)	0.073
C(B12)	−0.1722(31)	0.5161(19)	0.6927(22)	0.067	C(T8)	0.2838(31)	0.5421(18)	0.0243(16)	0.047
C(B13)	−0.1463(33)	0.5639(22)	0.6535(18)	0.063	O(3)	0.5549(20)	0.5418(10)	0.0787(10)	0.030
C(B14)	−0.0905(29)	0.6102(18)	0.6772(18)	0.039	C(T9)	0.4901(31)	0.5523(18)	0.1272(18)	0.056
C(1)	0.3592(32)	0.8418(18)	0.7521(16)	0.034	C(T10)	0.5638(42)	0.5844(22)	0.1669(21)	0.095
C(2)	0.4435(29)	0.8050(16)	0.7626(16)	0.032	C(T11)	0.6529(37)	0.5891(20)	0.1508(20)	0.082
C(3)	0.4735(29)	0.8029(17)	0.8243(18)	0.043	C(T12)	0.6597(32)	0.5614(17)	0.0911(17)	0.045
C(4)	0.4202(34)	0.8363(20)	0.8636(17)	0.055	O(4)	0.3138(40)	0.2723(23)	0.1864(25)	0.060
C(5)	0.3446(34)	0.8707(20)	0.8475(20)	0.067	C(T13)	0.2326(47)	0.2924(25)	0.1582(23)	0.060
C(6)	0.3102(28)	0.8767(18)	0.7870(18)	0.041	C(T14)	0.2900(50)	0.2703(27)	0.2403(27)	0.088
C(7)	0.1359(28)	0.7951(17)	0.5218(17)	0.024	C(T15)	0.1753(48)	0.2493(31)	0.1812(31)	0.119
C(8)	0.1029(31)	0.7662(16)	0.4718(16)	0.030	C(T16)	0.2083(54)	0.2414(30)	0.2422(29)	0.118
C(9)	0.0043(33)	0.7766(17)	0.4524(14)	0.030	O(5)	0.7067(23)	0.7089(14)	0.0182(15)	0.101
C(10)	−0.0582(27)	0.8130(17)	0.4830(17)	0.033	C(T17)	0.7349(33)	0.7148(21)	0.0757(21)	0.092
C(11)	−0.0104(35)	0.8368(17)	0.5361(18)	0.041	C(T18)	0.6778(34)	0.7637(24)	−0.0115(18)	0.096
C(12)	0.0845(35)	0.8309(17)	0.5549(16)	0.035	C(T19)	0.7649(33)	0.8084(19)	0.0141(19)	0.077
C(13)	0.4920(30)	0.6655(17)	0.5896(17)	0.030	C(T20)	0.7994(30)	0.7813(20)	0.0748(18)	0.074
C(14)	0.5736(33)	0.6366(20)	0.6202(17)	0.061	C(31)	0.6919(18)	−0.0970(36)	0.1221(15)	0.1627
C(15)	0.5996(30)	0.5820(19)	0.5945(19)	0.051	C(32)	0.6141(38)	−0.0754(73)	0.1722(29)	0.4220
C(16)	0.5476(33)	0.5636(18)	0.5400(19)	0.056	C(33)	0.9355(10)	−0.0219(18)	0.3768(08)	0.0463
C(17)	0.4742(33)	0.6027(22)	0.5135(18)	0.065	C(34)	0.9883(16)	−0.0705(31)	0.3597(13)	0.1299
C(18)	0.4412(30)	0.6567(18)	0.5366(19)	0.049	C(35)	0.8768(16)	−0.0807(31)	0.3696(13)	0.1289
C(19)	0.4114(27)	0.5928(18)	0.7061(15)	0.021	C(36)	0.9527(22)	−0.0303(42)	0.4323(18)	0.2079
C(20)	0.4420(35)	0.5353(22)	0.6952(18)	0.065	C(37)	0.9757(09)	0.4653(17)	0.3896(07)	0.0409
C(21)	0.5317(37)	0.5153(19)	0.7245(20)	0.065	C(38)	1.0048(11)	0.4278(21)	0.3457(09)	0.0690
C(22)	0.5812(32)	0.5532(23)	0.7625(19)	0.065	C(39)	0.9814(11)	0.5993(21)	0.3964(09)	0.0637
C(23)	0.5438(35)	0.6055(22)	0.7766(17)	0.065	C(40)	1.0016(09)	0.4021(19)	0.4374(08)	0.0489
C(24)	0.4544(31)	0.6314(17)	0.7456(18)	0.041	O(X1)	0.1413(18)	0.1831(37)	0.3729(16)	0.1103
C(25)	0.1442(25)	0.7746(16)	0.7628(16)	0.018	C(X1)	0.1730(22)	0.2734(46)	0.4805(18)	0.0772
C(26)	0.0899(27)	0.8082(17)	0.7234(15)	0.024	C(X3)	0.1502(22)	0.1728(45)	0.4661(18)	0.0700
C(27)	0.0264(34)	0.8550(21)	0.7441(2)	0.082	C(X3)	0.1108(20)	0.1959(39)	0.2860(17)	0.0580
C(28)	0.0278(30)	0.8642(18)	0.8025(19)	0.052	C(X4)	0.1416(23)	0.1243(45)	0.3284(20)	0.0767
C(29)	0.0823(31)	0.8294(19)	0.8424(17)	0.050	C(X5)	0.1731(26)	0.1413(50)	0.4222(22)	0.0909
C(30)	0.1500(26)	0.7821(17)	0.8241(16)	0.033					

[a] See footnote *a* in Table 2.

exchanged positions with a THF ligand. A remarkable feature of this coupling reaction, which very likely is entropically driven, is the displacement of a THF molecule by a μ_2-S^{2-} ligand in the coordination sphere of the highly oxophilic Zr^{IV} ion.

The Zr–B distances (Table 6) show that in both **I** and **II** three of the BH_4^- anions (B_1, B_3, B_4) serve as tridentate ligands and one (B_2) is bidentate. The Zr–B distances with the *tridentate* BH_4^- ligands at 2.344(8) and 2.29(2) Å, respectively, for **I** and **II** are very similar to the one known for $Zr(BH_4)_4$. In the latter complex, a low-temperature X-ray study[30] and an electron diffraction study[31] show the Zr–B distance at 2.34 and 2.308(3) Å, respectively. Zr–B distances of 2.368(6) and 2.39(2) Å also were reported for the η^3-BH_4^- ligands in the Zr polyhydride complexes $M_3H_6(BH_4)_6(PMe_3)_4$ and $M_2H_4(BH_4)_4(dmpe)_2$ that contain both η^2- and η^3-BH_4^- ligands.[32]

In **I** and **II** the Zr–B distances (for the η^2-BH_4^- ligands) at 2.53(2) and 2.512(12) Å, respectively, are shorter than the same type of distances in the Zr polyhydride complexes[33] at 2.633(4) and 2.70(1) Å but quite similar to the appropriate (η^2-BH_4^-) Zr–B distances in the $M_2H_3(BH_4)_5(PMe_3)_2$ complex[33] at 2.604(8) Å and the $(MeCp)_2Hf(BH_4)_2$ complex[34] at 2.553(6) Å.

The Zr(1) and Zr(2) atoms in **I** and **II** are formally eight coordinate and are coordinated by either tetrahydrofuran or BH_4^- terminal ligands. A common and unusual feature in both **I** and **II** is the presence of the formally nine-coordinate Zr(2) that

(30) Bird, P. H.; Churchill, M. R. *Chem. Commun.* **1967**, 403.
(31) (a) Spiridonov, V. P.; Mamawa, G. I. *J. Struct. Chem.* **1969**, *10*, 120. (b) Plato, V.; Hedberg, K. *Inorg. Chem.* **1971**, *10*, 590.
(32) Gozum, J. E.; Wilson, S. R.; Girolami, G. S. *J. Am. Chem. Soc.* **1992**, *114*, 9483–9492.
(33) Gozum, J. E.; Girolami, G. S. *J. Am. Soc.* **1991**, *113*, 3829.
(34) Johnson, P. L.; Cohen, S. A.; Marks, T. J.; Williams, J. M. *J. Am. Chem. Soc.* **1978**, *100*, 2709.

Table 6. Summary of Interatomic Distances[a] and Angles for $Zr_3S_3(^tBuS)_2(BH_4)_4(THF)_2$, **I**, $Zr_6S_6(^tBuS)_4(BH_4)_8(THF)_2{\cdot}2CH_2Cl_2$, **II**, $Zr_3(S)(^tBuS)_{10}{\cdot}^1/_2Et_2O$, **III**, and $(Mg(THF)_6)[Zr_2(SPh)_{7.2}(CH_2Ph)_{1.8}]_2{\cdot}3THF$, **IV**

	I[b]	II[c]	III[d]	IV[e]
		Distances		
Zr(1)–Zr(2)	3.278(2)	3.475(1)	3.732(2)	3.942(6) [3.942(6)]
Zr(1)–Zr(3)	3.564(2)	3.468(1)	3.720(2)	
Zr(2)–Zr(3)	3.574(2)	3.507(1)	3.714(2)	
Zr(1)–Zr(1′)		3.712(2)		
Zr(1)–S(1)	2.554(4)	2.641(2)		2.510(15) [2.509(13)]
Zr(1)–S(2)	2.620(4)	2.610(2)	2.600(5)	2.477(16) [2.493(13)]
Zr(1)–S(3)	2.450(4)	2.527(2)	2.606(5)	2.472(18) [2.497(14)]
Zr(1)–S(4)	2.645(4)	2.633(2)	2.771(5)	2.634(14) [2.633(12)]
Zr(1)–S(3′)		2.595(2)		
Zr(1)–S(5)	4.840(4)		2.597(5)	2.624(12) [2.632(10)]
Zr(1)–S(6)			2.439(5)	2.670(14) [2.691(12)]
Zr(1)–S(7)			2.425(5)	
Zr(2)–S(1)	2.563(4)	2.597(2)	2.660(7)	
Zr(2)–S(2)	2.635(4)	2.648(2)		
Zr(2)–S(3)	2.445(4)	2.616(2)	2.611(5)	
Zr(2)–S(4)			2.759(5)	2.712(14) [2.715(12)]
Zr(2)–S(5)	2.655(4)	2.658(2)	2.608(5)	2.762(12) [2.735(11)]
Zr(2)–S(6)				2.698(12) [2.708(11)]
Zr(2)–S(7)				2.463(16) [2.463(14)]
Zr(2)–S(8)			2.430(6)	
Zr(2)–S(9)			2.408(5)	
Zr(2)–S(X1)			2.647(13)	
Zr(2)–C(B1)				2.34(3) [2.36(3)]
Zr(2)–C(B8)				2.28(5) [2.33(4)]
Zr(2)–C(B2)				3.10(4) [3.13(4)]
Zr(2)–C(B9)				2.79(5) [2.76(4)]
Zr(3)–S(1)	2.634(4)	2.537(2)	2.679(7)	
Zr(3)–S(2)	2.555(4)	2.529(2)	2.604(5)	
Zr(3)–S(4)	2.634(4)	2.601(2)	2.766(5)	
Zr(3)–S(5)	2.630(4)	2.592(2)	2.600(5)	
Zr(3)–S(10)			2.400(5)	
Zr(3)–S(11)			2.443(6)	
Zr(3)–S(X1)			2.602(13)	
Zr(1)–O(1)	2.239(10)			
Zr(2)–O(2)	2.242(10)			
Zr(3)–O		2.295(6)		
Zr(1)–B(1)	2.35(2)	2.279(11)		
Zr(2)–B(2)	2.35(2)	2.511(11)		
Zr(2)–B(3)		2.325(11)		
Zr(3)–B(3)	2.33(2)			
Zr(3)–B(4)	2.53(2)	2.276(12)		
S(4)–C(1)	1.90(1)	1.892(9)		
S(5)–C(5)	1.85(2)	1.902(9)		
S–C			1.85(12,2)[a,f]	
B(3)–B(4)	3.52(3)			
Mg–O				2.14(3) [2.14(2)]
		Angles		
Zr–Zr(*i*)–Zr[f]	60(3,3.2)	60.0(3,3)	60.0(3,2)	
range	54.70(2)–62.80(2)	59.60(5)–60.70(5)	59.82(5)–60.33(5)	
Zr(*i*)–(μ_3-S)–Zr(*i*)[f]	84(6,2)	84.4(6,6)	91.3(3,2)	
range	77.2(1)–87.0(1)	82.8(1)–86.2(1)	91.0(2)–91.6(2)	
Zr(1)–S(3)–Zr(2)		85.0(1)		
Zr(1)–S(3)–Zr(1′)		92.9(1)		
Zr–(μ_2-S)–Zr	84.7(4)	83.4		
range	84.1(1)–85.1(1)	83.0(1), 83.8(1)		
Zr–(μ_2-RS)-Zr			90.2(3,1.3)	94.5(3,4) [94.4(3,4)]
range			88.1(2)–91.4(1)	94.1(4)–95.0(4)
S–Zr–S(cis)	80(15,1.5)	80(15,1.5)		
range	71.3(1)–87.3(1)	70.8(1)–89.2(1)		
S–Zr–S(trans)	150(3,3)	150(3,2)		
range	145.1(1)–153.5(2)	146.8(1)–152.7(1)		
S(3)–Zr(1)–S(3′)		87.1(1)		
B–Zr(*i*)–S(cis)[g]	103.5(5,6)			
range	102.8(6)–104.1(6)			
t-RS–Zr–t-RS			94.4(3,1.6)	84.7(3,6) [85.2(3,7)]
range			91.7(1)–95.9(1)	84.2(5)–85.6(6)
t-RS–Zr–μ_2-RS			101.3(12,1.4)	86.4(3,1.3) [86.3(3,1.3)]
range			95.1(1)–109.1(2)	85.2(5)–88.5(6)
t-RS–Zr–μ_2-RS(trans, prox)				126.7(3,6) [126.3(3,8)]
range				125.8(5)–127.5(5)
t-RS–Zr–μ_2-RS(trans, dist)				146.2(3,8) [146.4(3,8)]
range				145.6(5)–147.5(5)
t-RS–Zr–μ_3-RS(cis)			83.1(3,1.3)	
range			81.0(1)–84.4(1)	

Table 6 (Continued)

	I[b]	II[c]	III[d]	IV[e]
t-RS–Zr–μ_3-RS(trans)			174.5(3,1.4)	
range			172.7(2)–176.6(2)	
t-RS–Zr–μ_3-S(cis)			109(3,3)	
range			107.1(1)–114.0(1)	
t-RS–Zr–μ_3-S(trans)			155.4(3,1.2)	
range			154.3(2)–156.6(2)	
μ_2-RS–Zr–μ_3-RS			80(6,3)	
range			72.1(1)–84.8(1)	
μ_2-RS–Zr–μ_3-S			74(6,3)	
range			68.7(1)–83.9(1)	
μ_2-RS–Zr–μ_2-RS			145(3,4)	71.9(6,1.0) [72.0(6,1.8)]
range			138.7(2)–148.8(2)	69.4(4)–75.4(4)
μ_3-RS–Zr–μ_3-S			73.3(3,1)	
range			73.3(1)–73.2(1)	
B–Zr(*i*)–S(trans)[g]	174.5	170(4,5)		
range	173.9(5), 175.0(6)	158.8(3)–178.3(3)		
B(3)–Zr(3)–S(cis)	99(4,3)	100(12,2)[h]		
range	92.9(7)–107.9(5)	82.0(3)–109.8(4)		
O–Zr–S(cis)	88(6,2)	88(4,2)		
range	83.5(3)–92.6(3)	85.4(2)–91.9(4)		
O–Zr–S(trans)	162.0	165.7(2)		
range	162.1(3), 162.0(3)			
O–Zr–B	94.2	91.9(4)		
range	94.0(6), 94.4(6)			
B(3)–Zr(3)–B(4)	92.9(7)	96.9(5)[i]		
Zr–S–C(term)	119.4(4,6)			
range	118.6(6)–120.6(6)			
Zr–S–C(bridge)		121.0(4,3)		
range		120.5(3)–121.3(3)		
Zr–CB8–CB9				93(3) [88(2)]
Zr–CB1–CB2				105(3) [104(2)]

[a] Individual interatomic distances and mean values of crystallographically independent, chemically equivalent bond angles. The first number in parentheses represents the number of chemically equivalent bond angles averaged out; the second number represents the larger of the individual standard deviations or the standard deviation from the mean, σ, where $\sigma = (\sum_{i=1}^{N}(x_i - \bar{x})^2/N(N-1))^{1/2}$. [b] In **I**, the C–C bonds within the t-Bu groups of the t-BuS$^-$ ligands are in the range 1.48(2)–1.56(2) Å with a mean value of 1.52(2) Å; for the THF ligands the C–O bonds are in the range 1.34(3)–1.62(4) Å with a mean value of 1.49(5) Å; the C–C bonds are in the range 1.39(3)–1.60(5) Å with a mean value of 1.50(5) Å. [c] In **II**, the C–C bonds within the t-Bu groups of the t-BuS$^-$ ligands are in the range 1.49(2)–1.53(1) Å with a mean value of 1.507(15) Å; for the THF ligands the C–O bonds are in the range 1.37(5)–1.99(2) Å with a mean value of 1.57(9) Å; the C–C bonds are in the range 1.01(7)–1.92(6) Å with a mean value of 1.45(11) Å. [d] In **III**, for the t-Bu groups the C–C bonds are in the range 1.41(6)–1.57(2) Å with a mean value of 1.50(6) Å. [e] Bond lengths and angles reported in brackets were obtained from the structure solution using low-temperature (~−50 °C) data. In **IV**, (ambient-temperature data) for the thiophenolate ligands the C–S bonds are in the range 1.78(5)–1.88(5) Å with a mean value of 1.82(4) Å. The C–C bonds in the phenyl rings are the range 1.34(5)–1.51(5) Å with a mean value of 1.42(5) Å. For the benzyl ligands the two CH_2–Ph bonds are 1.55(4) and 1.56(4) Å and the C–C bonds within the phenyl rings are in the range 1.38(4)–1.47(4) Å with a mean value of 1.42(2) Å. In cation N1 the N–C bonds are in the range 1.51(1)–1.52(1) Å with a mean value of 1.51(1) Å; for the THF ligands in the $[Mg(THF)_6]^{2+}$ cation the C–O bonds are in the range 1.34(6)–1.59(6) Å with a mean value of 1.47(6) Å; the C–C bonds are in the range 1.32(7)–1.74(7) Å with a mean value of 1.52(7) Å. [f] Range 1.75(2)–1.90(2) Å; *i* and *j* cycle 1–3. [g] *i* = 1, 2. [h] B–Zr–S(cis). [i] B(2)–Zr(2)–B(3). Very similar values but with slightly smaller standard deviations are found in the structure solved with −50 °C data.

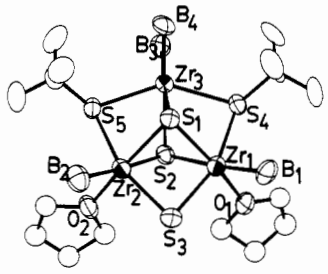

Figure 4. Structure and labeling of $Zr_3S_3(^tBuS)_2(BH_4)_4(THF)_2$, **I**. Thermal ellipsoids as drawn by ORTEP (Johnson, C. K. *ORNL-3794*; Oak Ridge National Laboratory: Oak Ridge, TN, 1965) represent the 40% probability surfaces.

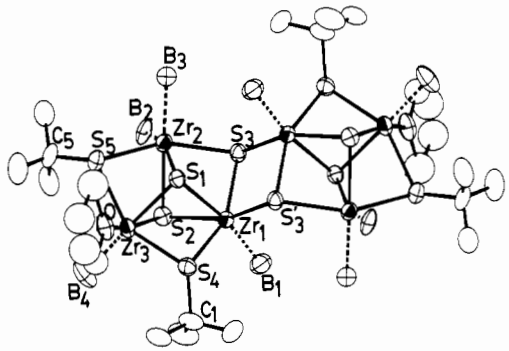

Figure 5. Structure and labeling of $Zr_6S_6(^tBuS)_4(BH_4)_8(THF)_2$, **II**. Thermal ellipsoids as drawn by ORTEP represent the 40% probability surfaces.

contains both bidentate and tridentate BH_4^- terminal ligands. The Zr atoms bound to only one BH_4^- ligand however contain the ligand in only the η^2 coordination mode. Although there exist numerous complexes that contain either bidentate or tridentate BH_4^- ligands,[35] **I** and **II** represent a less common class of complexes where the BH_4^- ligands display both modes of coordination within the same complex. Other compounds of this type are the previously mentioned hydride–borohydride–phosphine complexes.[32,33]

The basic core structure of the $Zr_3(S_{ax})_2$ units in **I** and **II** is geometrically similar but metrically different than the $Mo_3(S_{ax})_2$ unit in the $(Mo_3S_2Cl_9)^{3-}$ trianion.[36] In the latter, M–M bonding results in Mo–Mo distances nearly 1 Å shorter than the Zr–Zr distances in **I** or **II** (Table 6). The remarkable flexibility of the S^{2-} capping ligands in accommodating the widely different Mo_3

(35) James, B. D.; Wallbridge, M. G. H. *Prog. Inorg. Chem.* **1970**, *11*, 99.

(36) Huang, J.; Shang, M.; Lui, S.; Lu, J. *Sci. Sin. (Engl. Transl.)* **1982**, *25*, 1270.

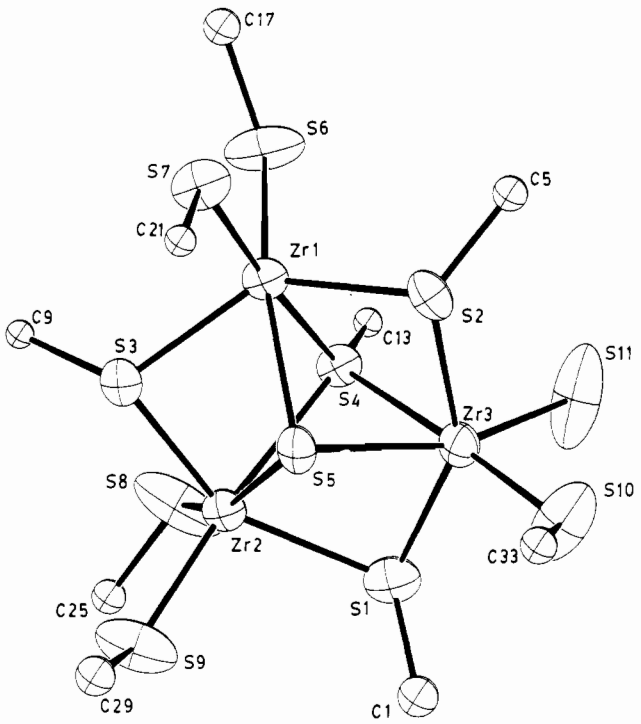

Figure 6. Structure and labeling of $Zr_3(S)(^tBuS)_{10}$, **III**. Thermal ellipsoids as drawn by ORTEP represent the 40% probability surfaces.

Table 7. Weighted Least-Squares Planes with Deviations from the Planes (Å) of Atoms used To Define the Planes and Dihedral Angles between Selected Planes

Zr_3 (I)

atom	plane 1	plane 2	plane	plane 4	plane 5
Zr(1)	−0.144(3)	0.093(4)			
Zr(2)	−0.149(3)		0.093(4)		
Zr(3)	−0.206(2)			0.002(4)	
S(1)		−0.073(4)	−0.073(3)	−0.002(5)	
S(2)		−0.086(3)	−0.086(4)	−0.002(4)	
S(3)	0.137(3)			0.002(4)	
S(4)	0.179(4)		0.066(3)		
S(5)	0.183(3)	0.065(4)			

Zr_6 (II)

atom	plane 1	plane 2	plane 3	plane 4	plane 5
Zr(1)	0.135(2)	0.023(3)			0.00
Zr(2)	0.040(1)		0.045(2)		
Zr(3)	0.330(2)			0.031(2)	
S(1)		−0.22(2)	−0.045(2)	−0.026(2)	
S(2)		−0.017(3)	−0.033(3)	−0.026(3)	
S(3)	−0.062(2)			0.020(2)	0.00
S(4)	−0.254(1)		0.032(2)		
S(5)	−0.189(1)	0.016(2)			
S(3′)[a]					0.00

Dihedral Angles (deg)

Zr_3 (I)

plane 1–plane 2	87.51	plane 2–plane 3	60.70
plane 1–plane 3	87.48	plane 2–plane 4	59.68
plane 1–plane 4	90.03	plane 3–plane 4	120.38

Zr_6 (II)

plane 1–plane 2	93.89	plane 2–plane 3	60.79
plane 1–plane 3	93.28	plane 2–plane 4	121.39
plane 1–plane 4	89.46	plane 3–plane 4	60.60
		plane 1–plane 5	60.20

[a] Primed atom is related to unprimed atom by the center of symmetry.

and Zr_3 triangular units in these clusters is illustrated in the M–S_b–M angles that vary from very acute (66.9°) in the Mo cluster to rather oblique values (84.1 and 84.4°) in **I** and **II**.

A comparison of the structural parameters of the cores in **I** and **II** to the one in **III** shows similar Zr–μ_3-S and Zr–μ_2-S distances but a wide variation in Zr–Zr distances (Table 6). The Zr–Zr distances in **I** and **II** at 3.47(12) and 3.48(2) Å and in **III** at 3.722(6) Å definitely are determined by predominant Zr–Zr repulsions, subject to steric considerations. A similar situation prevails in the structure of the $U_3(O)(^tBuO)_{10}$ cluster[28] with a U–U distance of 3.547(1) Å. The Zr–Zr distances within the Zr_3 triangular units in **I**–**III** correlate with the Zr–μ_2-S–Zr and Zr–μ_3-S–Zr angles. In **I** and **II** (with shorter Zr–Zr distances) these angles are 84.7(4), 83.4(1)° and 84(2), 84.4(6)°, respectively. In **III** (with longer Zr–Zr distances) these angles are more oblique at 90.2(1.3) and 91.3(2)°, respectively. By far the longest Zr–Zr distance is found in **IV** at 3.942(6) Å with a Zr–μ_2-S–Zr angle in this molecule of 94.5(4)° and a Zr–μ_2-S distance of 2.64(2) Å. The latter is similar to corresponding distances in **I**–**III** (Table 6).

The structure of **III** presents an opportunity to examine the bonding of a thiolate ligand bound in three different coordination modes within the same molecule. An expected monotonic increase in the Zr–S distances is observed (2.423(8), 2.617(7), 2.765(5) Å) as the coordination mode of the thiolate ligand changes from terminal to μ_2 to μ_3. This behavior has a precedent in the structures of the $(M_4(SR)_{10})^{2-}$ "adamantanes". In the latter the mean value of the M–S bonds with the six μ_2 bridging RS^- ligands invariably is larger than the value of the M–S bonds with the RS^- terminal ligands.[37-39] The very long Zr–μ_3-SR distances in **III** are nearly 0.3 Å longer than the sum of the Zr and S covalent radii (2.49 Å) and suggest that the μ_3-RS^- bridge may be a site of unusual reactivity. This reactivity has not been observed, and attempts to substitute the μ_3-SR ligand in **III** with other ligands have resulted in rapid decomposition.

The $[Zr_2(SPh)_7(CH_2Ph)_2]^-$ dimer in **IV** is the first example of an anionic zirconium thiolate complex. The structure (Figure 7) is best described in terms of the cofacial fusion between the triangular faces of *trigonal prismatic* ($Zr(1)(SR)_6$) and *octahedral* ($Zr(2)(SR)_4(CH_2Ph)_2$) subunits (Figure 8). The benzyl ligand C(B8)–C(B14) appears to bind to Zr(2) in a η^2 fashion with Zr(2)–C(B8) and Zr(2)–C(B9) bond lengths of 2.33(4) and 2.76(4) Å and a Zr(2)–C(B8)–C(B9) angle of 88(2)°. The small angle at the methylene carbon correlates with the close proximity of C(B9) to the metal and suggests that there is a some π interaction between the benzyl ligand and the Zr atom. This type of bonding interaction has been found previously in several benzyl complexes[40] including $Ti(CH_2Ph)_4$[41] and the cationic $[(Cp)_2Zr(CH_2Ph)(MeCN)]^+$ complex.[42] For the latter the Zr–CH_2 and the Zr–C(Ph) distances are 2.344(8) and 2.648(6) Å and the Zr–CH_2–C(Ph) angle is 84.9(2)°.

The other benzyl ligand in **IV** (C(B1)–C(B7)) is bound to Zr(2) in a similar fashion; however, it occupies the site at 80% occupancy with the remaining 20% contributed by a thiophenolate ligand. In the distorted trigonal prismatic $Zr(1)(SR)_6$ unit the two triangular faces are rotated by 14.5° from a totally eclipsed orientation. In the $Zr(2)(SR)_4(CH_2Ph)_2$ unit the midpoints between the H_2C–CPh carbons of the η^2-benzyl ligands and the four PhS^- ligands define a distorted octahedron. The distortions of the two units from idealized trigonal prismatic or octahedral geometries are mainly attributed to the differences in the Zr–S bond lengths between terminal and bridging thiophenolate ligands. The mean values of the Zr(1)–μ_2-S and Zr(2)–μ_2-S bonds at

(37) Costa, T.,; Dorfman, J. R.; Hagen, K. S.; Holm, R. H. *Inorg. Chem.* **1983**, *22*, 4091.
(38) Dance, I. G. *J. Am. Chem. Soc.* **1979**, *101*, 6264.
(39) Coucouvanis, D.; Kanatzidis, M.; Simhon, E.; Baenziger, N. C. *J. Am. Chem. Soc.* **1982**, *104*, 1874.
(40) (a) Davis, G. R.; Javris, J. A.; Piols, P. J. *J. Chem. Soc., Chem. Commun.* **1971**, 677. (b) Latesky, S. L.; McMullen, A. K.; Rothwell, I. P.; Huffman, J. C. *Organometallics* **1985**, *4*, 902.
(41) Bassi, J. W.; Allegra, C.; Scordamaglia, R.; Chioccola, G. *J. Am. Chem. Soc.* **1971**, *93*, 3787.
(42) (a) Jordan, R. F.; LaPointe, R. E.; Bajgur, C. S.; Echols, S. F.; Willet, R. *J. Am. Chem. Soc.* **1987**, *109*, 4113. (b) Jordan, R. F. *J. Chem. Educ.* **1988**, *65*, 285.

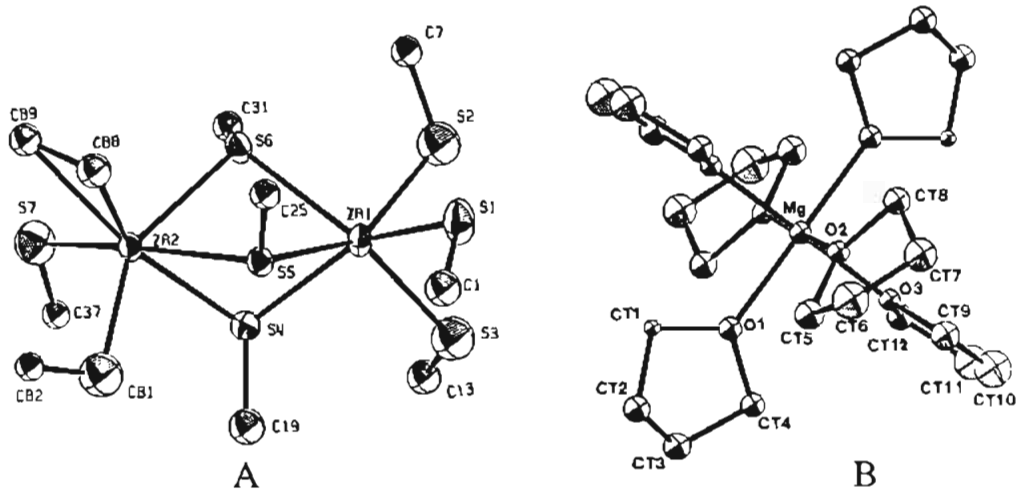

Figure 7. Structure and labeling of $(Mg(THF)_6)[Zr_2(SPh)_{7.2}(CH_2Ph)_{1.8}]_2 \cdot 3THF$, **IV**. Thermal ellipsoids as drawn by ORTEP represent the 40% probability surfaces. (A) represents the dimeric $Zr_2(SPh)_{7.2}(Bz)_{1.8}$ monoanion, and (B) represents the $(Mg(THF)_6)^{2+}$ counterion.

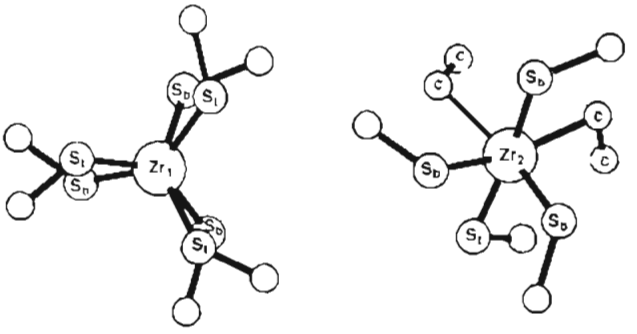

Figure 8. The two, individual six-coordinate zirconium subunits in the $Zr_2(SPh)_7(CH_2Ph)_2$ dimer as viewed with the Zr–Zr vector perpendicular to the plane of the paper.

2.64(2) and 2.72(1) Å are significantly longer than the Zr(1)–S_t and Zr(2)–S_t bonds of 2.50(1) and 2.46(1) Å. The μ_2-S–Zr–μ_2-S and S_t–Zr–S_t angles at 72(1) and 85(1)°, respectively, compensate for the differences in the Zr–S bond lengths and result in nearly equidimensional $(S_t)_3$ and $(\mu_2\text{-S})_3$ triangular faces. The Zr–Zr distance in **IV** at 3.942(6) Å is long and represents the distance where the Zr–Zr and μ_2-SR–μ_2-SR repulsions are at a minimum. The U(IV) dimer $[U_2(^t\text{BuO})_9]^-$, structurally characterized as the K^+ salt,[43] possesses a face-sharing bioctahedral structure and also shows a long U–U separation of 3.631(2) Å.

(43) Cotton, F. A.; Marler, D. O.; Schwotzer, W. *Inorg. Chem.* **1984**, *23*, 4211–4215.

Summary and Conclusions

The synthesis of extremely oxygen and moisture sensitive Zr thiolate complexes is accomplished readily from either $Zr(BH_4)_4$ or $Zr(CH_2Ph)_4$ in reactions with aliphatic or aromatic thiols in nonpolar solvents. These reactions are essentially acid–base reactions where the Zr-coordinated BH_4^- or $(CH_2Ph)^-$ ligands react with the mildly acidic protons of the thiols to generate B_2H_6 and CH_3Ph, respectively. The thiolate anions generated in these reactions coordinate to the Zr atoms. Aliphatic thiolate ligands such as $^t\text{BuS}^-$, which can generate stable carbonium ions, undergo what appears to be mainly heterolytic C–S bond cleavage with the generation of S^{2-} ligands. In the structures of the $Zr_3S_3(^t\text{BuS})_2(BH_4)_4(THF)_2$, **I**, $Zr_6S_6(^t\text{BuS})_4(BH_4)_8(THF)_2$, **II**, and $Zr_3(S)(^t\text{BuS})_{10}$, **III**, clusters the S^{2-} anions serve as doubly or triply bridging ligands. The dimeric $(Mg(THF)_6)[Zr_2(SPh)_{7.2}(CH_2Ph)_{1.8}]_2 \cdot 3THF$ complex, **IV**, does not contain S^{2-} ligands and reflects the comparative superior stability of the C–S bond in aromatic thiolate ligands. In **IV** this bond does not undergo a cleavage reaction to generate S^{2-} ligands.

Acknowledgment. The support of this work by a grant (CH-83-0389) from the National Science Foundation is gratefully acknowledged.

Supplementary Material Available: Listings of hydrogen positional and thermal parameters, anisotropic thermal parameters, and bond distances and angles for $Zr_3S_3(^t\text{BuS})_2(BH_4)_4(THF)_2$, **I**, $Zr_6S_6(^t\text{BuS})_4(BH_4)_8(THF)_2$, **II**, $Zr_3(S)(^t\text{BuS})_{10}$, **III**, and $(Mg(THF)_6)[Zr_2(SPh)_{7.2}(CH_2Ph)_{1.8}]_2 \cdot 3THF$, **IV** (Tables S1–S4) (15 pages). Ordering information is given on any current masthead page. Crystallographic reflection intensity data for **I** and **II** have been deposited with ref 13, and that for **III**, with ref 14.